Supplementary materials to: Recent observations and glacier modeling point towards near complete glacier loss in western Austria (Ötztal and Stubai mountain range) if 1.5°C is not met

Lea Hartl[1, 2, *], Patrick Schmitt[3, *], Lilian Schuster[3], Kay Helfricht[1, 4], Jakob Abermann[5], and Fabien Maussion[3, 6]

[1]Institute for Interdisciplinary Mountain Research, Austrian Academy of Sciences, Austria
[2]Alaska Climate Research Center, Geophysical Institute, University of Alaska Fairbanks, USA
[3]Department of Atmospheric and Cryospheric Sciences, University of Innsbruck, Austria
[4]Hydrological Service Tyrol, Office of the Tyrolean Government, Austria
[5]Department of Geography and Regional Science, Graz University, Austria
[6]School of Geographical Sciences, University of Bristol, Bristol, UK
[*]These authors contributed equally to this work.

Correspondence: Lea Hartl (lea.hartl@oeaw.ac.at), Patrick Schmitt (patrick.schmitt@uibk.ac.at)
These authors contributed equally to the work and share first authorship.

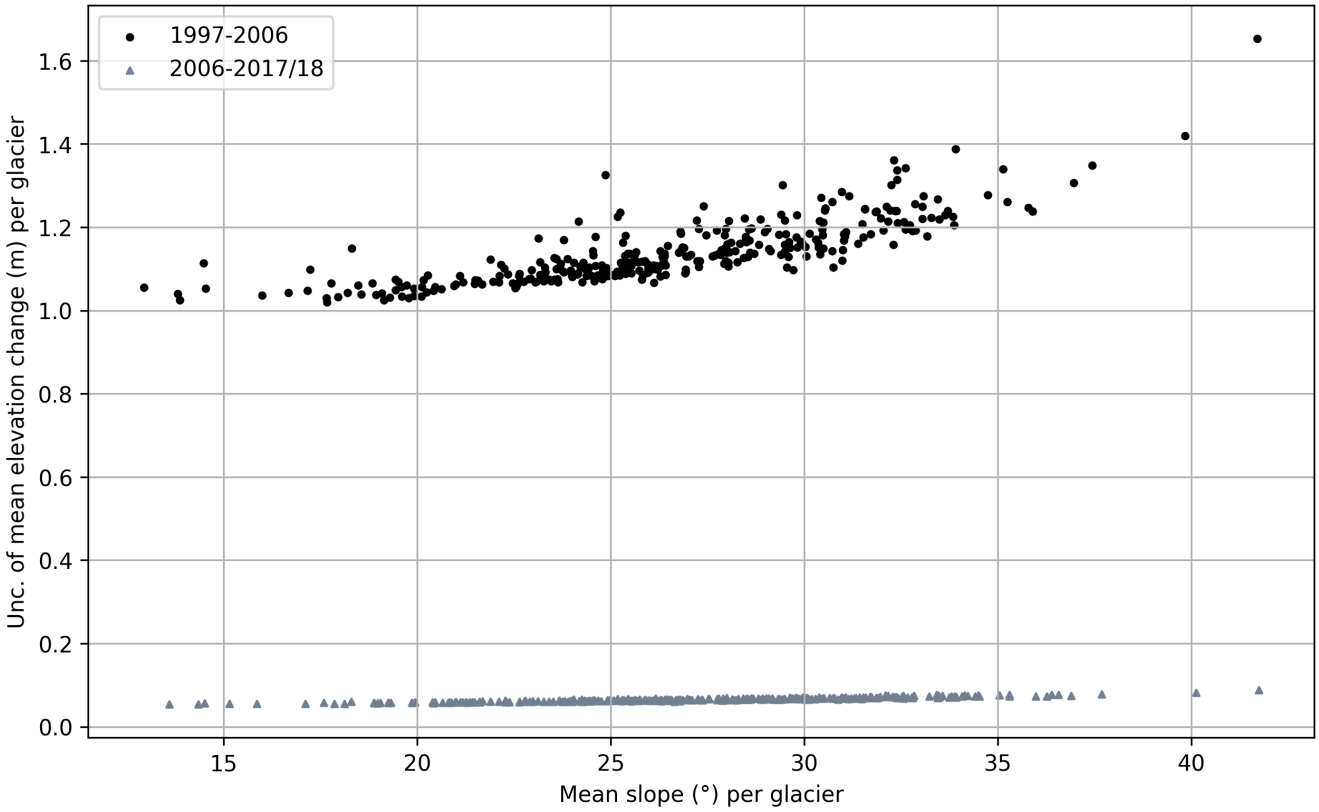

Figure S1. Uncertainty of mean elevation change for each glacier in the study area computed from spatially propagated elevation errors, for the periods 1997-2006 and 2006-2017/18. Uncertainty is plotted against the mean slope angle of the corresponding glaciers.

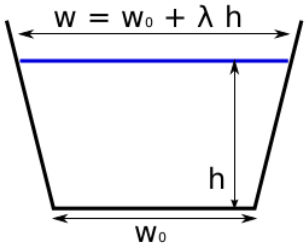

Figure S2. Trapezoidal shape with two degrees of freedom. The width change with thickness depends on λ. The angle β of the side wall (as defined from the horizontal plane, i.e. λ = 0 -> β = 90°) is defined by $\beta = atan\frac{2}{\lambda}$. Taken from https://docs.oggm.org/en/v1.6.1/ice-dynamics.htmltrapezoidal.

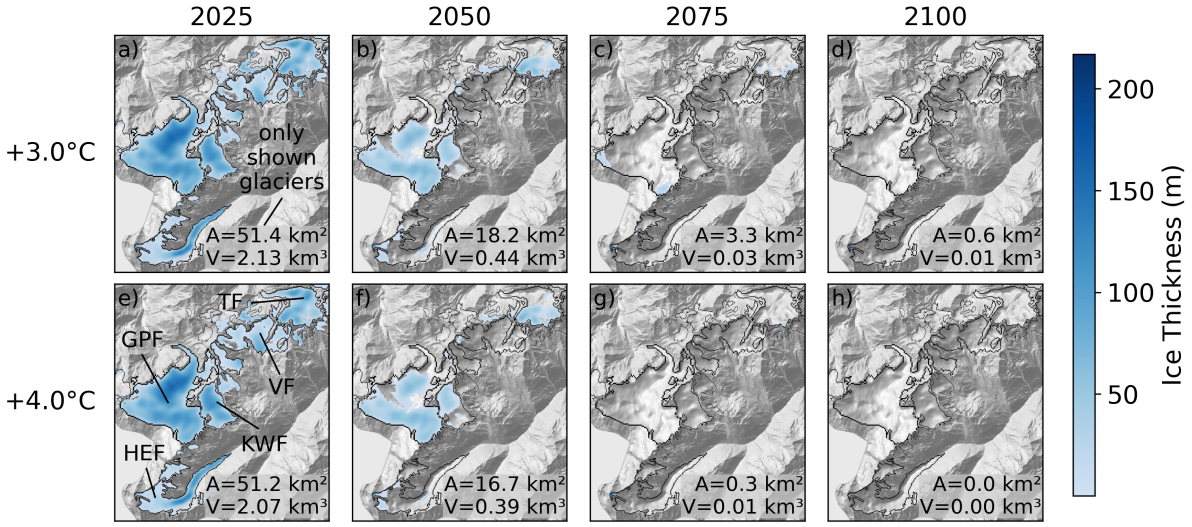

Figure S3. Projected ice distribution across 27 glaciers in a subset of the ROI, including Hintereisferner (HEF), Kesselwandferner (KWF), Vernagtferner (VGF) Taschachferner (TSF) and Gepatschferner (GPF) for a +3.0°C warming scenario (a, b, c and d) and a +4°C warming scenario (e, f, g and h). The figure shows single models which are closest to the ensemble median volume (see Table S4). For each subfigure, the total area (A) and the total volume (V) of the 27 glaciers are noted in the bottom right corner. Shades of blue represent the ice thickness at each grid point. The 2017 outlines are shown in black.

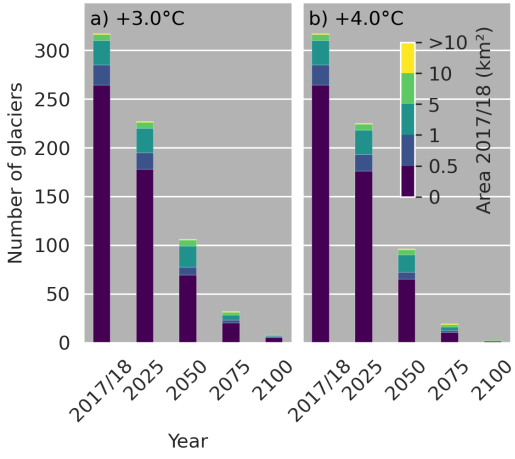

Figure S4. The projected future changes in the number of glaciers under +3.0°C (a) and +4.0°C (b) scenarios, illustrated by single models which are closest to the ensemble median volume (see Table S4). Colors represent area size classes in 2017/18 (see Table **??**).

Table S1. Volume change rates and uncertainties (see Section 2.2 in the main manuscript) for different periods and different source data.

Source	Coverage	Spatial resolution	Glacier outlines used for extraction	Period	Volume change ($km^3\ yr^{-1}$)	Mean elevation change (m yr^{-1})	Normalized median absolute deviation (NMAD, m)
GI2, GI3	Regional	5m x 5m	GI2 (1997)	1997-2006	-0.1722±0.026	-0.84± 0.126	0.315*
GI3, 2017/18	Regional	5m x 5m	GI3 (2006)	2006-2017/18	-0.1710±0.005	-0.92± 0.009	0.017*
Hugonnet et al. (2021)	Global	100m x 100m	Extracted for RGI boundaries (2003) within ROI.	2000-2020	-0.1699	-0.96	0.021**

*stable terrain outside GI1 boundaries, **stable terrain outside RGI boundaries

Table S2. Global glacier projection studies and input data sets used.

Data type	Data citation/source	Citing studies				
		OGGM v1.6.1	Zekollari et al. (2019)	Rounce et al. (2023)	Compagno et al. (2021)	Cook et al. (2023)
Glacier area/ boundaries	RGI (RGI6, Pfeffer et al. (2014))	X	X	X	X	X
Digital elevation models	NASADEM (NASA JPL (2020))	X		X		
	SRTM v.4 (Jarvis et al. (2008))		X		X	
	COPDEM 2022 (COP (2022))					X
Geodetic mass balance	Hugonnet et al. (2021)	X		X		X
	WGMS data 2018		X			
	Zemp et al. (2019)				X	
Ice thickness data	Farinotti et al. (2019)	X		X	X	

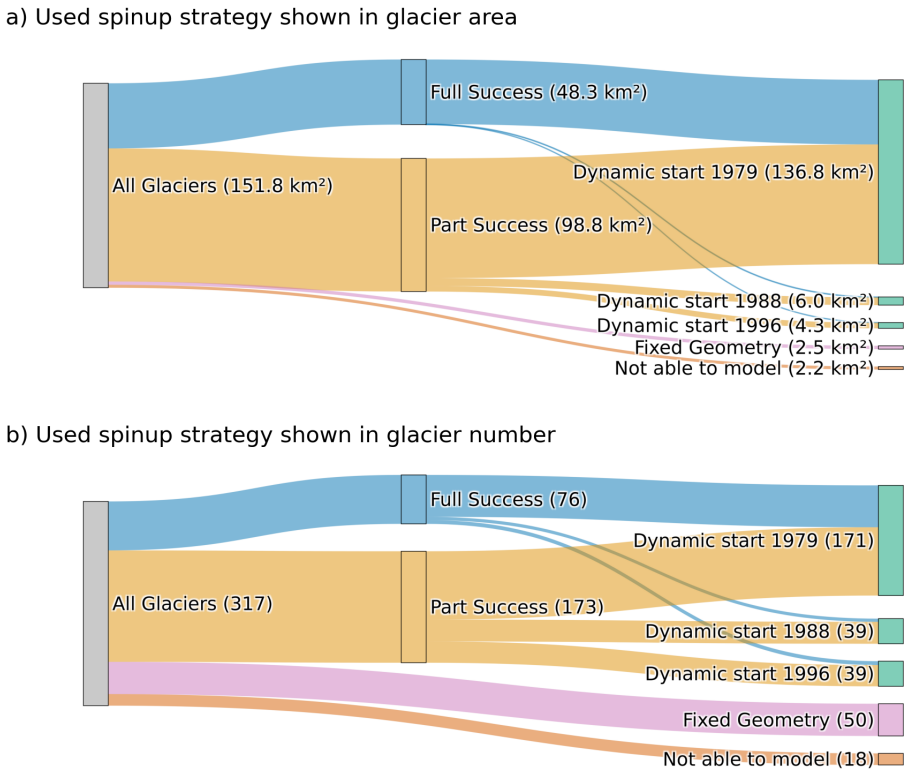

Figure S5. Overview of the used calibration strategy of OGGM regional in terms of total area of our ROI (a) and in terms of glacier number of our ROI (b). 'All Glaciers' (grey bar) represents the 2017/18 outline observations. At the right, the green bars are all glaciers which used a dynamic spinup, purple bars used a fixed geometry spinup and the red bars were not able to be modelled. The individual outcomes of the dynamic spinup calibration are described in more detail in Appendix A.

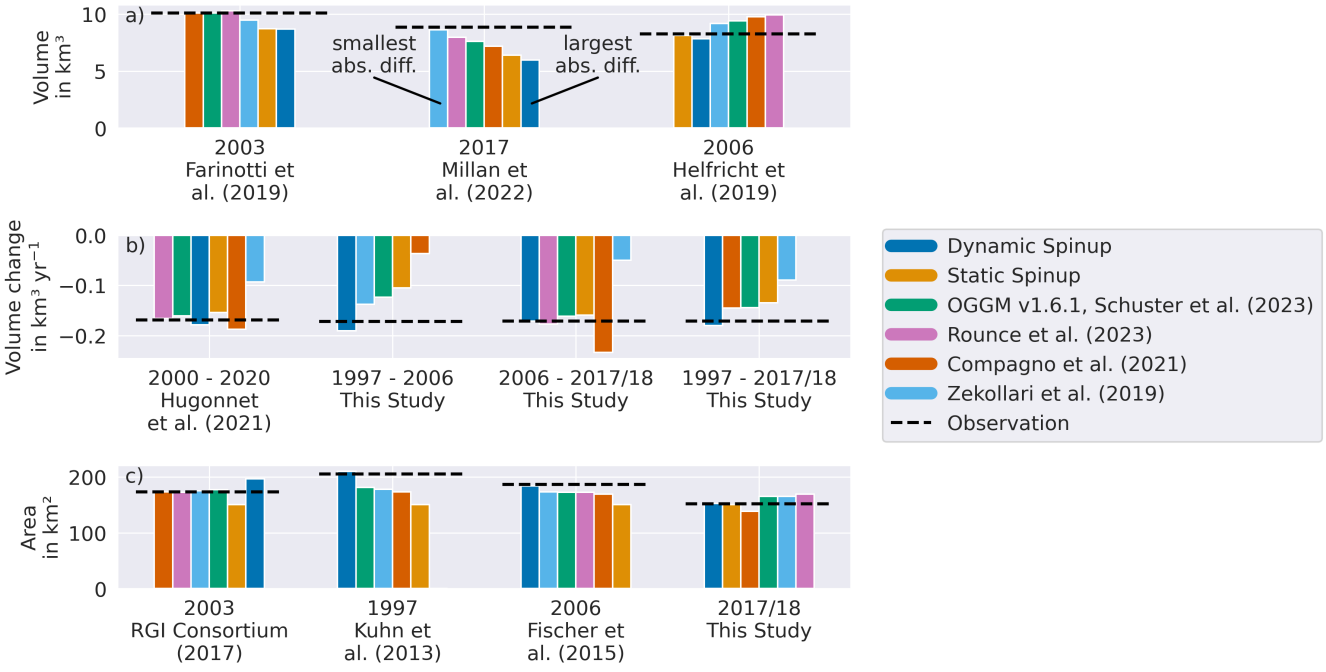

Figure S6. Comparison of model values from various studies with a) volume estimates in km^3, b) volume change observations in km^3 yr^{-1}, and c) area in km^2. The x-axis labels show the year corresponding to the estimate/observation and the related publication. The actual estimate/observation is represented by a dashed black line. Individual model values are depicted with colored bars. These bars are sorted based on their absolute difference from the estimate/observation, with the smallest absolute difference (best fit) on the left and the largest (least fit) on the right. An overview of which datasets where used by which study for calibration can be found in Table S2 and the corresponding values can be found in Table S3.

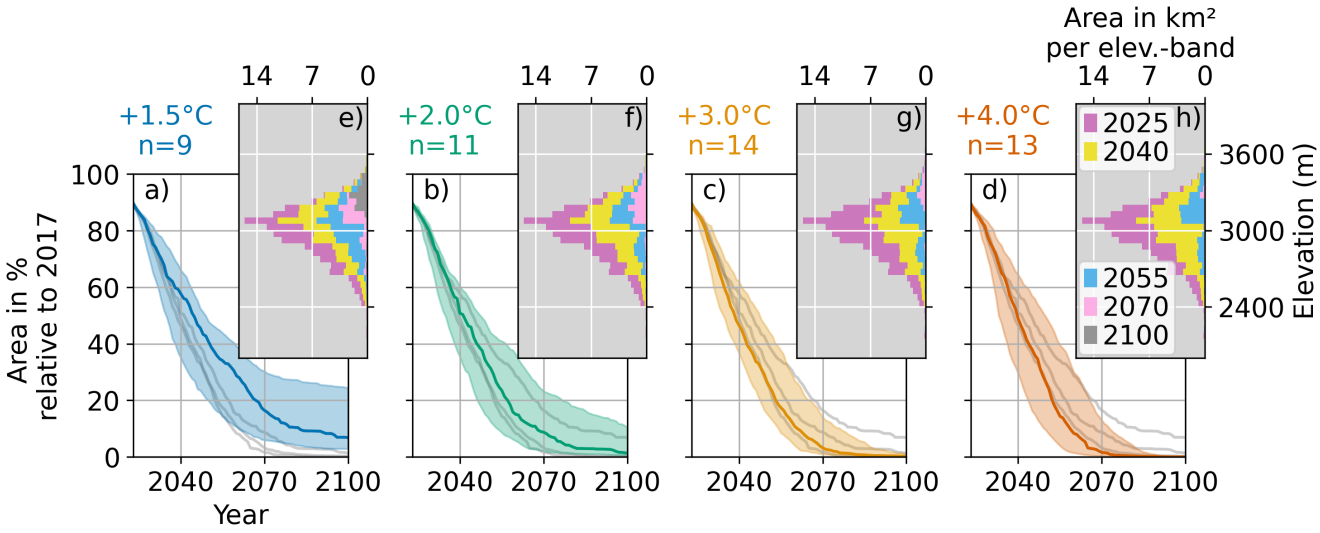

Figure S7. Median (colored lines) and 5th and 95th percentile (shading) of the OGGM regional projections per future global temperature scenario as percentage of 2017 glacier area in the ROI (a, b, c and d). The grey lines in each subplot show the median of the other three scenarios for reference. Temperature increase and number of climate model realizations n per scenario stated above the volume evolution plots. Insets (e, f, g and h) show the distribution of ice area per 50 m elevation bands in different years for the four temperature scenarios, for the model run closest to the volume median of the scenario ensemble (see Table S4).

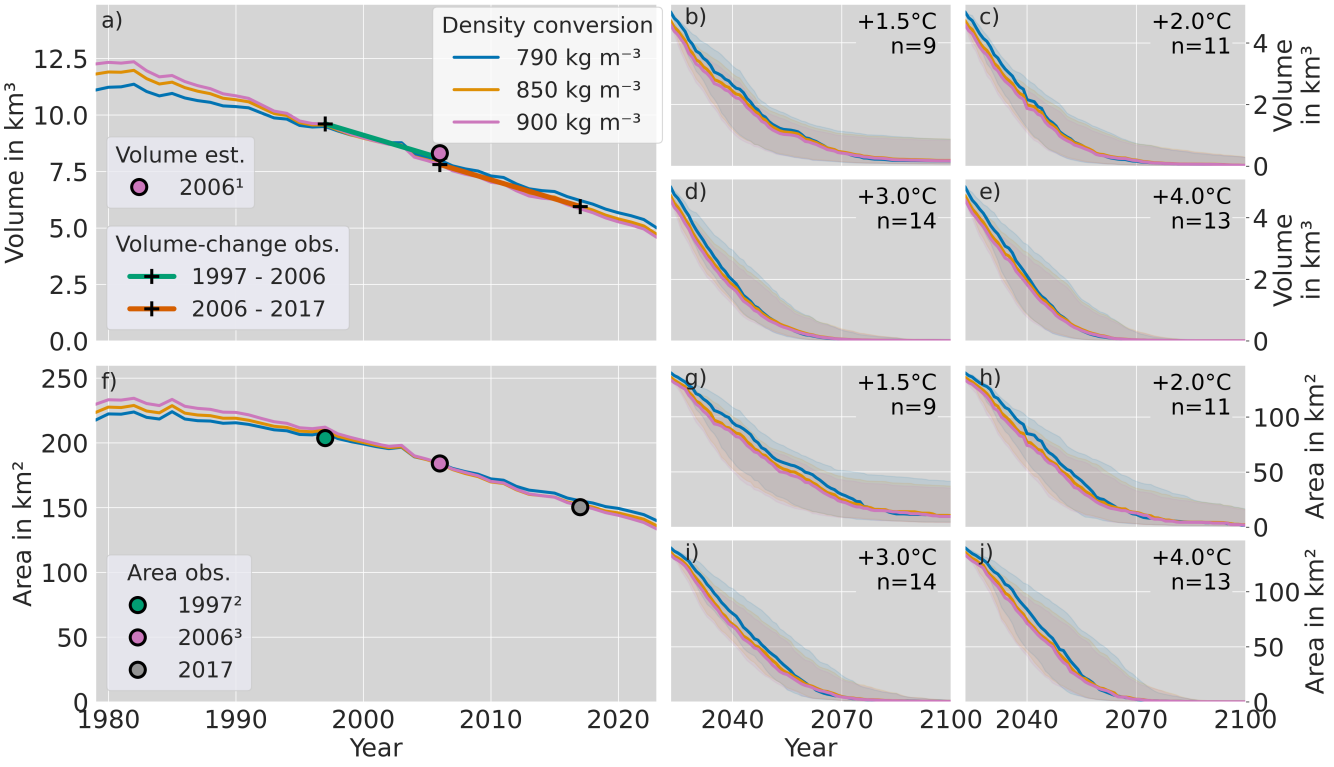

Figure S8. Shows the influence on volume and area for the past and the future of using density conversion factors of 790 kg m^{-3}, 850 kg m^{-3} and 900 kg m^{-3} for converting the observed volume change into an observed mass changed, which is used during the dynamic calibration outlined in Appendix A. The range of these three values mirrors the range given in Huss and Farinotti (2012). In the past period we do not see much influence from the different conversion factors. However, in the near future projections we see a slower glacier decline when using 790 kg m^{-3} compared to the other two. This effect vanishes around 2060 for the volume and 2070 for the area and has no big influence on the date when the baseline volume (0.18 km^3) is crossed.

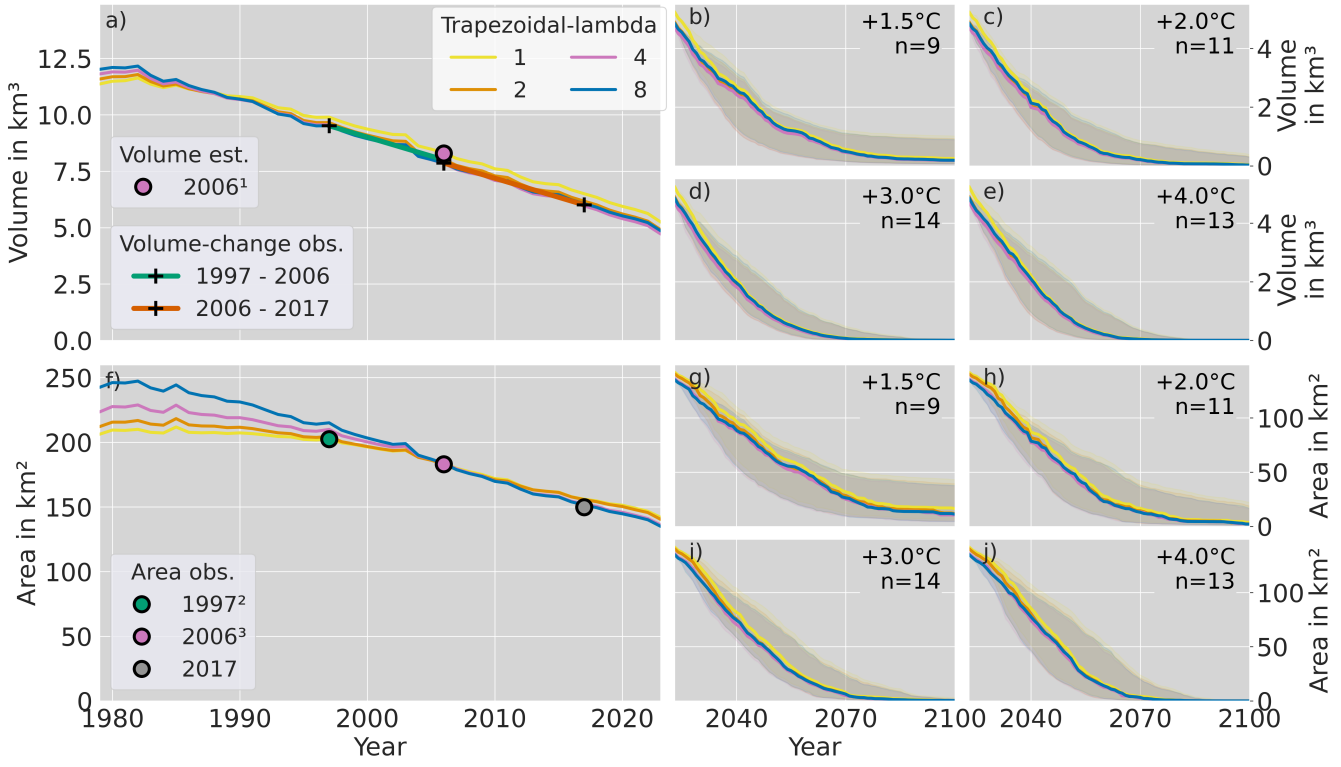

Figure S9. Shows the influence of different trapezoidal cross-section angels λ (defined in S2) on volume and area for the past and the future for four different scenarios. The volume change and the area 2006 are matched by all, as part of the dynamic calibration methodology (outlined in Section **??**). However, the resulting area evolution depends on the defined value of λ. Best agreement in simultaneously matching the area 2006 and 2017 was found for a value of 4. For future projections, we see differences mainly in the near future but no big influence on the timing of when the baseline volume (0.18 km^3) is crossed. Zekollari et al. (2019) also noted improved area matching with a wall angle close to λ=4. However, they retained the default value of 2 due to the minimal impact of λ on projections, which our assessment confirms. Nevertheless, optimizing lambda could be important to consider for potential future reanalysis studies of glacier change in the past.

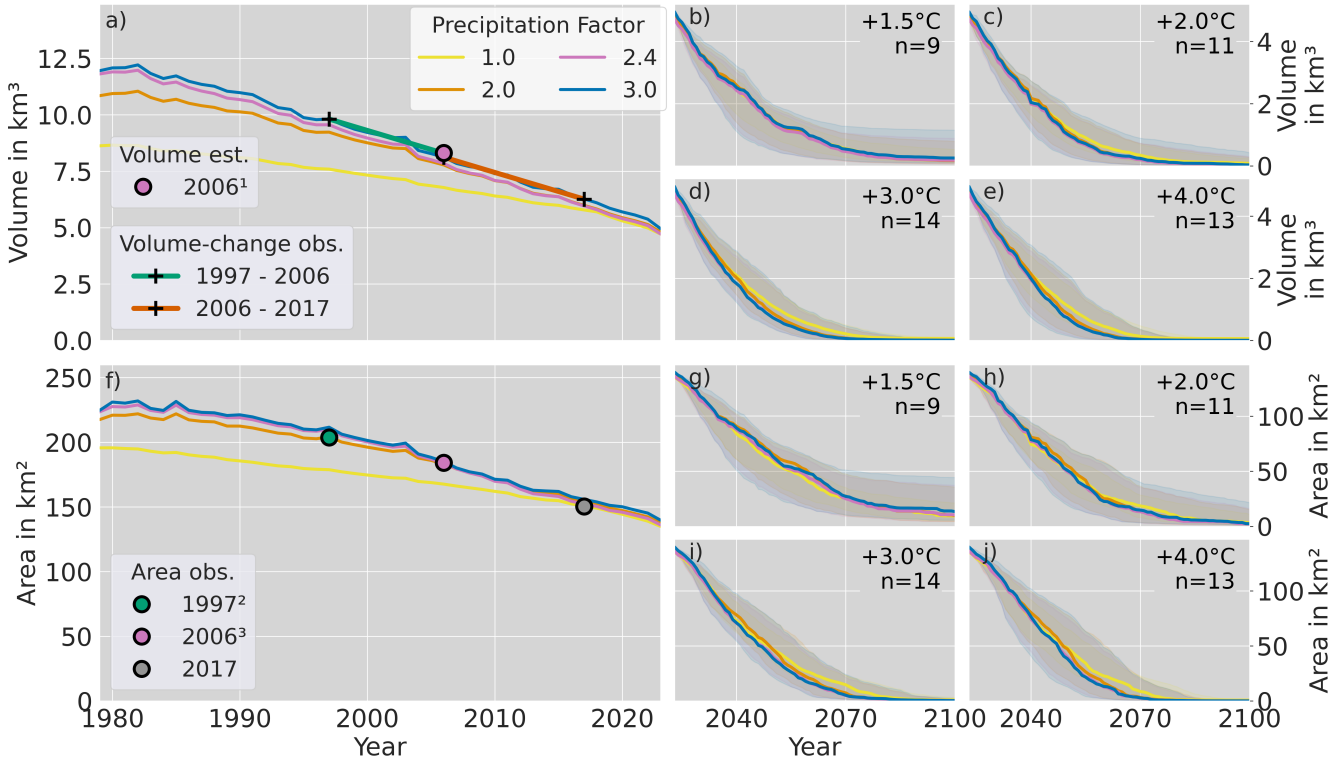

Figure S10. Shows the influence on volume and area in the past and future for four different precipitation factors 1, 2, 2.4 and 3. Looking at the past area of precipitation factor 1 we see a clear mismatch of earlier areas. This could be attributed to the inability of the dynamic spinup to find a glacier state in the past which evolves into the glacier area 2006 and therefore it falls back to a static spinup (explained in detail in Appendix A). The dynamic spinup fails because of too little accumulation, and the algorithm tries to compensate for this by growing very big glaciers for the initialisation year 1979, which exceed the domain boundaries and therefore fail. For future projections, beside of +1.5°C, we see slower glacier melting between the period 2040 and 2070 for precipitation factor 1. In contrast the factors 2, 2.4 and 3 look very similar in the past and the future. Additional estimates of glacier volume in the past could help to further constrain this. However, we decided to use 2.4 as described in Section 2.4.1

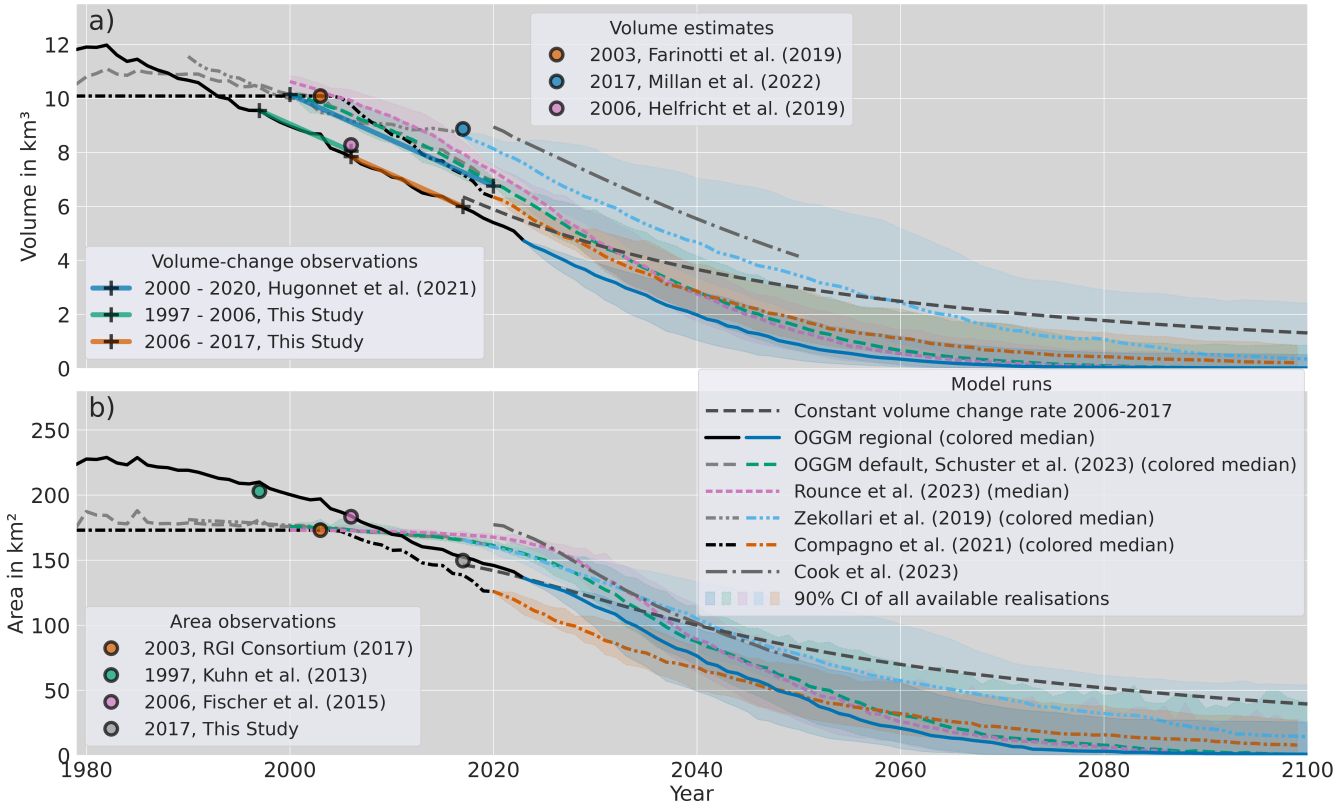

Figure S11. Total volume (a) and area (b) evolution in the ROI between 1979 and 2100 for constant volume change rate 2006-2017, OGGM regional, OGGM default (Schuster et al., 2023a), Rounce et al. (2023), Zekollari et al. (2019), Compagno et al. (2021) and Cook et al. (2023). For future periods the median (colored line) with the 5th to 95th percentile range (90% Confidence Interval (CI)) is shown, for all available realisations of the individual studies. For Cook et al. (2023) only the realisiation using a linearly interpolated observed mass balance trend is included. Further included are global datasets and regional datasets used by individual studies for calibration. Global datasets consist of volume estimates from Farinotti et al. (2019) and Millan et al. (2022), volume-change observations from Hugonnet et al. (2021), and area observations from Randolph Glacier Inventory Consortium (2017). Regional datasets consist of a volume estimate from Helfricht et al. (2019), volume-change observations from 1997-2006 and 2006-2017 as part of this study, and area observations from Kuhn et al. (2013), Fischer et al. (2015) and one at 2017 as part of this study.

Table S3. Shows the observed values for volume (km^3), volume-change (km^3 yr^{-1}) and area (km^2) along the corresponding values of the different models compared in the study. The same values are used in Figure S6.

	Observed	OGGM regional	OGGM v1.6.1 (Schuster et al., 2023b)	Rounce et al. (2023)	Compagno et al. (2021)	Zekollari et al. (2019)
Volume (km^3)						
2003	10.3[1]	8.7	10.1	10.3	10.1	9.5
2017	9.28[2]	6.0	7.6	8.0	7.2	8.6
2006	8.45[3]	7.9	9.4	9.9	9.8	9.2
Volume change (km^3 yr^{-1})						
2000-2020	-0.170[4]	-0.180	-0.161	-0.165	-0.187	-0.093
1997-2006	-0.172	-0.192	-0.123	—-	-0.036	-0.137
2006-2017	-0.171	-0.174	-0.162	-0.177	-0.234	-0.050
1997-2017	-0.171	-0.182	-0.145	—-	-0.145	-0.089
Area (km^2)						
1997	205.1[6]	210.0	181.0	—-	173.0	178.2
2003	173.1[7]	197.0	177.6	172.9	173.0	175.0
2006	186.6[8]	183.9	172.9	172.6	169.0	173.0
2017	151.8	152.3	165.5	169.5	138.6	165.6

1: Farinotti et al. (2019), 2: Millan et al. (2022), 3: Helfricht et al. (2019), 4: Hugonnet et al. (2021), 5: Patzelt (2013), 6: Kuhn (2013), 7: RGI Consortium (2017), 8: Fischer et al. (2015a)

Table S4. Model realisations used for the different global temperature increase scenarios (+1.5°C, +2°C, +3°C and +4.0°C) comparing the period 2071-2100 to preindustrial levels (1850-1900) as defined in IPPC (2019). Temperature limits were defined to get a representative number of models for each category, so that the total mean of all models in a category is close to the target value. The model realization shown in bold is the one closest to the median 2023–2100 volume of OGGM regional across all model realizations for a given temperature scenario. This model is used in Figures 7 and 8 in the main manuscript and supp. Figures S3 and S4 as the representative run for each temperature scenario.

Temperature increase	Temperature limits	Model realisations	Mean total temperature increase
+1.5 °C	1.2 - 1.75 °C	EC-Earth3-Veg - SSP1-1.9; GFDL-ESM4 - SSP1-1.9; MRI-ESM2-0 - SSP1-1.9; FGOALS-f3-L - SSP1-2.6; GFDL-ESM4 - SSP1-2.6; **INM-CM4-8 - SSP1-2.6**; INM-CM5-0 - SSP1-2.6; MPI-ESM1-2-HR - SSP1-2.6; NorESM2-MM - SSP1-2.6	1.57 °C
+2 °C	1.75 - 2.5 °C	BCC-CSM2-MR - SSP1-2.6; CESM2 - SSP1-2.6; CESM2-WACCM - SSP1-2.6; EC-Earth3 - SSP1-2.6; EC-Earth3-Veg - SSP1-2.6; GFDL-ESM4 - SSP2-4.5; INM-CM4-8 - SSP2-4.5; INM-CM5-0 - SSP2-4.5; MPI-ESM1-2-HR - SSP2-4.5; MRI-ESM2-0 - SSP1-2.6 **NorESM2-MM, SSP2-4.5**	2.21 °C
+3 °C	2.5 - 3.5 °C	BCC-CSM2-MR - SSP2-4.5; CESM2 - SSP2-4.5; CESM2-WACCM - SSP2-4.5; EC-Earth3 - SSP2-4.5; EC-Earth3-Veg - SSP2-4.5; FGOALS-f3-L - SSP2-4.5; FGOALS-f3-L - SSP3-7.0; GFDL-ESM4 - SSP3-7.0; INM-CM4-8 - SSP3-7.0; **INM-CM5-0 - SSP3-7.0**; INM-CM5-0 - SSP5-8.5; MPI-ESM1-2-HR - SSP3-7.0; MRI-ESM2-0 - SSP2-4.5; NorESM2-MM - SSP3-7.0	3.08 °C
+4 °C	3.5 - 4.5 °C	BCC-CSM2-MR . SSP3-7.0; BCC-CSM2-MR . SSP5-8.5; CESM2 - SSP3-7.0; CESM2-WACCM - SSP3-7.0; EC-Earth3 - SSP3-7.0; EC-Earth3-Veg - SSP3-7.0; FGOALS-f3-L - SSP5-8.5; GFDL-ESM4 - SSP5-8.5; INM-CM4-8 - SSP5-8.5; MPI-ESM1-2-HR - SSP5-8.5; MRI-ESM2-0 - SSP3-7.0; MRI-ESM2-0 - SSP5-8.5; **NorESM2-MM . SSP5-8.5**	3.91 °C

References

Copernicus DEM, https://doi.org/10.5270/esa-c5d3d65, 2022.

Compagno, L., Eggs, S., Huss, M., Zekollari, H., and Farinotti, D.: Brief communication: Do 1.0, 1.5, or 2.0° C matter for the future evolution of Alpine glaciers?, The Cryosphere, 15, 2593–2599, 2021.

Cook, S. J., Jouvet, G., Millan, R., Rabatel, A., Zekollari, H., and Dussaillant, I.: Committed Ice Loss in the European Alps Until 2050 Using a Deep-Learning-Aided 3D Ice-Flow Model With Data Assimilation, Geophysical Research Letters, 50, https://doi.org/10.1029/2023gl105029, 2023.

Farinotti, D., Huss, M., Fürst, J. J., Landmann, J., Machguth, H., Maussion, F., and Pandit, A.: A consensus estimate for the ice thickness distribution of all glaciers on Earth, Nature Geoscience, 12, 168–173, https://doi.org/10.1038/s41561-019-0300-3, 2019.

Fischer, A., Seiser, B., Stocker-Waldhuber, M., and Abermann, J.: The Austrian Glacier Inventory GI 3, 2006, in ArcGIS (shapefile) format, https://doi.org/10.1594/PANGAEA.844985, 2015.

Helfricht, K., Huss, M., Fischer, A., and Otto, J.-C.: Calibrated ice thickness estimate for all glaciers in Austria, Frontiers in Earth Science, 7, 68, 2019.

Hugonnet, R., McNabb, R., Berthier, E., Menounos, B., Nuth, C., Girod, L., Farinotti, D., Huss, M., Dussaillant, I., Brun, F., and Kääb, A.: Accelerated global glacier mass loss in the early twenty-first century, Nature, 592, 726–731, https://doi.org/10.1038/s41586-021-03436-z, 2021.

Huss, M. and Farinotti, D.: Distributed ice thickness and volume of all glaciers around the globe, Journal of Geophysical Research: Earth Surface, 117, n/a–n/a, https://doi.org/10.1029/2012jf002523, 2012.

IPPC: The Ocean and Cryosphere in a Changing Climate: Special Report of the Intergovernmental Panel on Climate Change [H.-O. Po¨rtner, D.C. Roberts, V. Masson-Delmotte, P. Zhai, M. Tignor, E. Poloczanska, K. Mintenbeck, A. Alegría, M. Nicolai, A. Okem, J. Petzold, B. Rama, N.M. Weyer (eds.)], Cambridge University Press, https://doi.org/10.1017/9781009157964, 2019.

Jarvis, A., Guevara, E., Reuter, H., and Nelson, A.: Hole-filled SRTM for the globe : version 4 : data grid, published by CGIAR-CSI on 19 August 2008., 2008.

Kuhn, M., Lambrecht, A., and Abermann, J.: Austrian glacier inventory 1998 (GI II), https://doi.org/10.1594/PANGAEA.809196, 2013.

Millan, R., Mouginot, J., Rabatel, A., and Morlighem, M.: Ice velocity and thickness of the world's glaciers, Nature Geoscience, 15, 124–129, https://doi.org/10.1038/s41561-021-00885-z, 2022.

NASA JPL: NASADEM Merged DEM Global 1 arc second V001, https://doi.org/10.5067/MEASURES/NASADEM/NASADEM_HGT.001, 2020.

Pfeffer, W. T., Arendt, A. A., Bliss, A., Bolch, T., Cogley, J. G., Gardner, A. S., Hagen, J.-O., Hock, R., Kaser, G., Kienholz, C., Miles, E. S., Moholdt, G., Mölg, N., Paul, F., Radić, V., Rastner, P., Raup, B. H., Rich, J., and and, M. J. S.: The Randolph Glacier Inventory: a globally complete inventory of glaciers, Journal of Glaciology, 60, 537–552, https://doi.org/10.3189/2014jog13j176, 2014.

Randolph Glacier Inventory Consortium: Randolph Glacier Inventory 6.0, https://doi.org/10.7265/N5-RGI-60, 2017.

Rounce, D. R., Hock, R., Maussion, F., Hugonnet, R., Kochtitzky, W., Huss, M., Berthier, E., Brinkerhoff, D., Compagno, L., Copland, L., Farinotti, D., Menounos, B., and McNabb, R. W.: Global glacier change in the 21st century: Every increase in temperature matters, Science, 379, 78–83, https://doi.org/10.1126/science.abo1324, 2023.

Schuster, L., Rounce, D. R., and Maussion, F.: Glacier projections sensitivity to temperature-index model choices and calibration strategies, Annals of Glaciology, pp. 1–16, https://doi.org/10.1017/aog.2023.57, 2023a.

Schuster, L., Schmitt, P., Vlug, A., and Maussion, F.: OGGM/oggm-standard-projections-csv-files: v1.0, https://doi.org/10.5281/ZENODO.8286064, 2023b.

Zekollari, H., Huss, M., and Farinotti, D.: Modelling the future evolution of glaciers in the European Alps under the EURO-CORDEX RCM ensemble, The Cryosphere, 13, 1125–1146, https://doi.org/10.5194/tc-13-1125-2019, 2019.

Zemp, M., Huss, M., Thibert, E., Eckert, N., McNabb, R., Huber, J., Barandun, M., Machguth, H., Nussbaumer, S. U., Gärtner-Roer, I., Thomson, L., Paul, F., Maussion, F., Kutuzov, S., and Cogley, J. G.: Global glacier mass changes and their contributions to sea-level rise from 1961 to 2016, Nature, 568, 382–386, https://doi.org/10.1038/s41586-019-1071-0, 2019.